

Basic research at GSI for the transmutation of nuclear waste

A. Kelić¹, P. Armbruster¹, L. Audouin², J. Benlliure³, M. Bernas², A. Boudard⁴,
 E. Casarejos³, S. Czajkowski⁵, L. Donadille⁴, T. Enqvist¹, B. Fernandez⁴,
 K. Helariutta¹, B. Jurado¹, R. Legrain⁴, S. Leray⁴, B. Mustapha², P. Napolitani^{1,2},
 J. Pereira³, M. Pratikoff⁵, F. Rejmund², M. V. Ricciardi¹, K.-H. Schmidt¹,
 C. Stéphan², J. Taïeb², L. Tassan-Got², C. Villagrasa⁴, F. Vives¹, C. Volant⁴,
 W. Wlazio⁴, O. Yordanov¹

1) GSI, Planckstraße 1, D-64291 Darmstadt, Darmstadt, Germany

2) IPN Orsay, IN2P3, F-91406 Orsay, France

3) University of Santiago de Compostela, E-15706 Santiago de Compostela, Spain

4) DAPNIA/SPhN CEA/Saclay, F-91191 Gif-sur-Yvette, France

5) CENBG, IN2P3, F-33175 Gradignan, France

a.kelic@gsi.de

Abstract: In the course of the concerted action “Lead for ADT”, which preceded the HINDAS project [1], an innovative experimental method has been developed at GSI-Darmstadt. This new approach is based on the inverse-kinematics method where a liquid-hydrogen target is bombarded with heavy projectiles. The reaction products are identified in-flight in mass and atomic number in a high-resolution spectrometer. Using this technique, we could detect, identify unambiguously and analyse about thousand nuclides per system before radioactive disintegration with an accuracy in the order of 10% to 15% in most cases. Moreover, thanks to the high-precision measurements of the velocity of the final residues, we could determine by which mechanism (spallation-fission or spallation-evaporation) they were produced.

The investigated systems provide stringent constraints to nuclear-reaction codes, in particular to the energy deposition in spallation, the modelling of the fission competition and the nuclide production in fission and on the energy dependence of spallation reactions. The new data will help to develop improved models with better predictive power for spallation reactions involving nuclei spanning a wide mass range.

Introduction

While the nuclear reactions occurring in a conventional fission reactor are limited to the energy range of fission neutrons below a few MeV, the nuclear reactions occurring in an accelerator-driven system, consisting of a sub-critical reactor and a neutron source driven by 1 GeV protons, extend to energies up to the primary proton energy. In addition to the detailed understanding of the neutronics and the complex transport phenomena of light particles, the production of heavy residues by proton- and neutron-induced fragmentation and fission reactions needs to be known for the design of such a system. This has decisive consequences for the shielding and the activation of the installation, the radiation damages of construction materials and the chemical properties of the spallation target. In contrast to the situation in conventional fission reactors, where all relevant nuclear data could be measured, the large range of energy and the variety of target materials involved in an accelerator-driven system demands for a different strategy. Only a limited number of selected key reactions can be studied in full detail and serve to benchmark, improve and develop nuclear-reaction codes, which are then used to calculate the reactions occurring in the accelerator-driven system in their full variety.

The conventional experiments on residual-nuclide production in proton- and neutron-induced reactions are performed by bombarding various target materials with protons or neutrons of the energy of interest and by analysing the produced species after irradiation, e.g. by their radioactive decay or by off-line and on-line mass spectrometry [2,3,4,5,6,7,8,9]. These methods can only give a limited insight into the reaction mechanism, because short-lived products, which form the dominant production in most cases, cannot be observed due to the time delay between the irradiation and the measurement. Information on the reaction kinematics is also not easily accessible. In addition, stable nuclides could only be detected with much effort e.g. by off-line mass spectrometry. As documented in a comprehensive intercomparison [10], the experimental information was not sufficient to develop reliable

models. In the course of the concerted action “Lead for ATD”, which preceded the HINDAS project, an innovative experimental method has been developed, which copes with this problem. This new approach is based on the bombardment of a hydrogen target with heavy projectiles. That means that the experiment is performed in inverse kinematics. The reaction products are identified in-flight in mass and atomic number in a high-resolution spectrometer. At the same time, information on the reaction kinematics is available. Using this technique, during the HINDAS project large sets of new experimental data with unprecedented quality have been accumulated [11].

In this paper, we report on the experimental and theoretical campaign dedicated to the studies of spallation reactions in the inverse kinematics. Most of the experimental results have been published in scientific journals [12,13,14,15]. Others are documented in PhD theses [16,17,18,19,20] and will be published soon. A comprehensive overview of the project and the obtained results can be found in Ref. [21].

Experiment

The experimental method and the analysis procedure have been developed and applied in previous experiments [22,23,24,25]. The heavy-ion synchrotron SIS at GSI, Darmstadt, can deliver the primary beams at energies between 0.2 – 1.5 A GeV. The dedicated experimental set up is shown in Fig. 1. The proton target was composed of 87.3 mg/cm² liquid hydrogen [13] enclosed between thin titanium foils of a total thickness of 36 mg/cm² [26]. The primary-beam intensity was continuously monitored by a beam-intensity monitor based on secondary-electron emission [27,28]. In order to subtract the contribution of the target windows from the measured reaction rate, measurements were repeated with the empty target. Heavy residues produced in the target were all strongly forward focused due to the inverse kinematics and the high velocity of the incoming beam. They were identified using the Fragment Separator (FRS) [29] and the associated detector equipment.

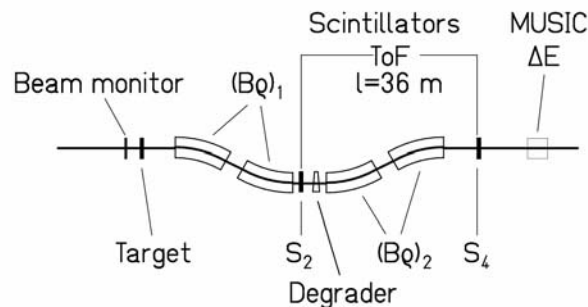


Figure 1. Schematic drawing of the fragment separator FRS with the detector equipment. For details see text.

The FRS is a two-stage magnetic spectrometer with a dispersive intermediate image plane (S_2) and an achromatic final image plane (S_4), with a momentum acceptance of 3% and an angular acceptance of about 15 mrad around the beam axis. Two position-sensitive plastic scintillators placed at S_2 and S_4 , respectively, provided the magnetic-rigidity ($B\rho$) and time-of-flight measurements, which allowed determining the mass-over-charge ratio of the particles. For an unambiguous isotopic identification of the reaction products, the analysis was restricted to ions, which passed both stages of the fragment separator fully stripped. The losses in counting rate due to the fraction of incompletely stripped ions and the losses due to secondary reactions in the layers of matter in the beam line were corrected for [13].

To identify all residues in the whole nuclear-charge range up to the projectile, it was necessary to use two independent methods in the analysis. The nuclear charges of the lighter elements, mainly produced by fission, were deduced from the energy loss in an ionisation chamber (MUSIC) with a resolution $Z/\Delta Z \approx 200$ obtained for the heaviest residues. Combining this information with the mass-over-charge ratio, a complete isotopic identification was performed. A mass resolution of $A/\Delta A \approx 400$ was achieved. Since part of the heavier reaction products was not completely stripped, the MUSIC signal was not sufficient for an unambiguous Z identification. Therefore, the identification of reaction products of heavier elements was performed with the help of an achromatic energy degrader [30] placed at the intermediate

image plane of the FRS. Degraded thicknesses of about 5 g/cm^2 of aluminium were used. The nuclear charge of the products was deduced from the reduction in magnetic rigidity by the slowing down in the energy degrader [13]. The MUSIC signal was still essential for suppressing events of incompletely stripped ions and from nuclei destroyed by secondary reactions in the degrader. The velocity of the identified residue was determined at S_2 from the $B\rho$ value and transformed into the frame of the beam in the middle of the target, taking into account the appropriate energy loss. In this way, the relative uncertainty in the velocity was about $5 \cdot 10^{-4}$. More than 100 different values of the magnetic fields were used in steps of about 2 % in order to cover all the produced residues and to construct the full velocity distribution of each residue in one projectile-target combination.

The re-construction of the full velocity distribution allows for disentangling reaction products formed in fragmentation and fission reactions due to their different kinematic properties. The velocity distribution as a function of neutron number for ${}_{30}\text{Zr}$ of one of the first system investigated, ${}^{238}\text{U}+{}^{208}\text{Pb}$ at 1 A GeV [23], is shown in Fig. 2 as cluster plot. It can be seen from the distribution that the reaction products can be attributed to different reaction mechanisms, i.e. fragmentation and fission. For isotopes produced by fission, only those emitted either in forward or in backward direction with respect to the primary beam can be observed in a given setting of the FRS because the angular acceptance is too small for sideward-emitted fragments [31].

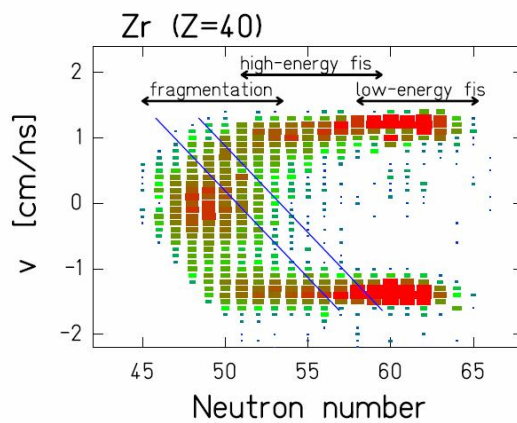


Figure 2. Velocity distributions of ${}_{40}\text{Zr}$ isotopes produced in the reaction ${}^{238}\text{U} + \text{Pb}$ at 1 A GeV [23]. The velocities are given in the projectile frame and have been corrected for the energy loss of the projectile and fragments in the target. Different contributions from different production mechanisms – fragmentation, high-energy fission and low-energy fission – can be distinguished due to the velocity and the neutron content of the fragments. For one setting of the FRS only events between the two blue lines are transmitted.

Cross sections and recoil velocities

The production of residual nuclides has been investigated for several systems, which are particularly relevant for the design of accelerator-driven systems: ${}^{56}\text{Fe}+{}^1\text{H}$ at 0.2 - 1.5 A GeV [16,19], ${}^{136}\text{Xe}+{}^1\text{H},\text{Ti}$ at 0.2 – 1 A GeV [19], ${}^{197}\text{Au}+{}^1\text{H}$ at 0.8 A GeV [24,25], ${}^{208}\text{Pb}+{}^1\text{H},\text{Ti}$ at 0.5 and 1 A GeV [18,17,13,32], ${}^{238}\text{U}+{}^1\text{H},\text{Ti}$ at 1 A GeV [14,15,20]. For each system, the production rates were measured for more than thousand nuclides. The velocity distributions of all these nuclides were determined at the same time. As an example, Figure 3 left shows the measured production cross sections from the reaction ${}^{208}\text{Pb}+{}^1\text{H}$ at 1 A GeV [13,32]. The different regions on the chart of the nuclides produced by spallation-evaporation and by spallation-fission reactions, respectively, can clearly be distinguished.

The experimental set up allows determining the recoil-velocity properties of the produced nuclei. For the spallation-evaporation residues, the velocity distributions are well represented by Gaussian distributions. The mean values of the recoil-velocity distribution were determined for each ion. The slowing down in the target area, assuming that the nuclear reaction occurred in the middle of the target on the average, was accounted for. In Figure 4a are plotted the mean velocities normalised following the prescriptions of Morrissey [33] for systems ${}^{238}\text{U}+{}^1\text{H}$ and ${}^{208}\text{Pb}+{}^1\text{H}$. Thus, we introduce p'_{\parallel} , which is the longitudinal recoil momentum, normalized in the following way [33]: $p'_{\parallel} = v_{\parallel} * M_p^* (\beta\gamma/(\gamma+1))$. This normalisation allows an inter-comparison of various measurements realised at different projectile energies. Figure 4a also includes the empirical systematics stated by Morrissey [33], which predicts a linear dependence between the reduced recoil momentum (p'_{\parallel}) and the mass loss (relative to the mass of the projectile). We observe that the systematics describes reasonably well the measured data.

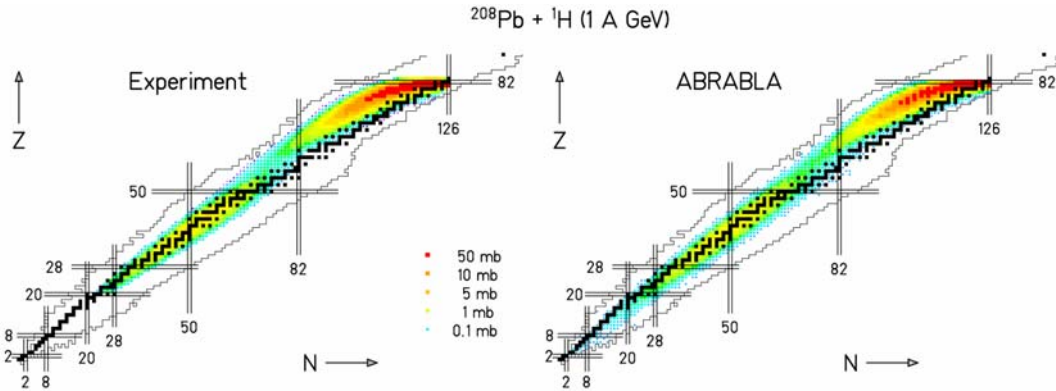


Figure 3: Residual nuclide cross sections measured in the experiment (left) and calculated with the ABRABLA code (right) for the reaction $^{208}\text{Pb} + ^1\text{H}$ at 1 A GeV shown on a chart of the nuclides. Nuclei with atomic number below 20 were not covered by the experiment.

The mean velocity values induced in the fission process are shown in Figure 4b for the same systems. The velocity values are obtained from the plots similar to Figure 2, averaged over the mass and corrected for the effect of the finite angular acceptance of the FRS. All fission velocities are consistent with the binary decay of a heavy nuclear system between lead and uranium for the $^{238}\text{U} + ^1\text{H}$ reaction, and between hafnium and lead in the case of the $^{208}\text{Pb} + ^1\text{H}$ reaction. The strong variation of the fission velocity with the atomic number of the fission fragment is mostly given by momentum conservation.

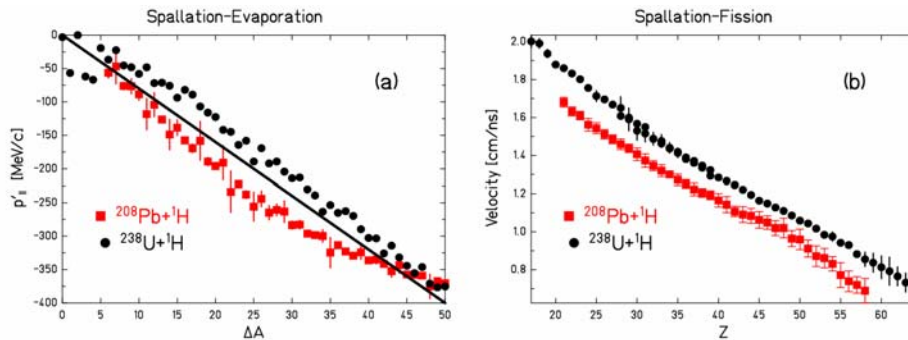


Figure 4: Mean recoil momentum induced in the spallation-evaporation of ^{238}U (black dots) and ^{208}Pb (red squares) by 1 GeV protons as a function of mass loss. The experimental data are compared with the systematics of Morrissey [33] (full line). (b) Measured mean velocities of the fission fragments produced for the same systems as a function of the atomic number of the fission fragments. The velocities are transformed into the frame of the beam.

Comparison with model calculations

In a spallation reaction, it is standard to distinguish between two separate stages. The first stage is usually modelled by individual nucleon-nucleon collisions with intra-nuclear-cascade codes, which ends with the formation of a thermalised excited nuclear system. The second stage is described in the statistical model of nuclear reactions. Several evaporation codes have been developed for this purpose. However, since most of these codes have been designed for fusion reactions, there is specific need for a code adapted to the deexcitation process of spallation residues: The large range of excitation-energies and the large variety of nuclear species demands for a consistent treatment of level densities as a function of excitation energy and nuclear shape. Due to the low angular momentum induced in spallation reactions, approximations which have been used for fusion reactions are not adapted. The dynamics of the fission process and the onset of thermal instabilities at the highest temperatures have to be considered. This demands for an explicit treatment of nuclear dynamics as a function of time. Modelling of fission requires considering a large variety of fissioning nuclei in a wide range of excitation energies. Available empirical formulations of nuclide distributions in fission of specific nuclei should be replaced by a model, which is based on more fundamental properties, like the potential energy landscape around saddle

and scission. Finally, the application in complex transport codes demands for short computing times.

The ABRABLA [34,35,36,37] code, developed at GSI and improved during the HINDAS project, satisfies these demands. As an example, in Figure 3 (right) the calculated nuclide production cross sections are compared with those measured in the reaction of $^{208}\text{Pb}+^1\text{H}$ at 1 A GeV. The length and the shape of the evaporation corridor are very well described by the calculations. The same is true for the competition between particle evaporation and fission. The correct description of the fission process is not only important for calculating the nuclide production in the spallation-fission reaction but also in the spallation-evaporation reaction. This is nicely seen in Figure 5 showing the mass distribution from the reaction $^{238}\text{U}+^1\text{H}$ at 1 A GeV. On the left side of the figure, the experimental data [14,15,20] are compared with the ABRABLA calculations taking explicitly into account the relaxation process in deformation space and the resulting time-dependent fission width based on an analytical approximation [37] to the solution of the Fokker-Planck equation. The agreement between the data and the calculations is more than satisfactory. On the contrary, if fission is treated as a pure statistical phenomenon [38] the calculation deviates strongly from the data, and this can be seen on the right part of Figure 5. If one would compare the total fission cross section measured in this reaction – (1.53 ± 0.2) b, with calculations based on the transition-state model – 1.73 b, one could be misled to conclude that this model is giving a good agreement with the measured data. But, the comparison with the spallation-evaporation mass distribution clearly shows that the transition-state model is not the proper description of the nuclear deexcitation, and that, consequently, fission has to be treated as a dynamical process.

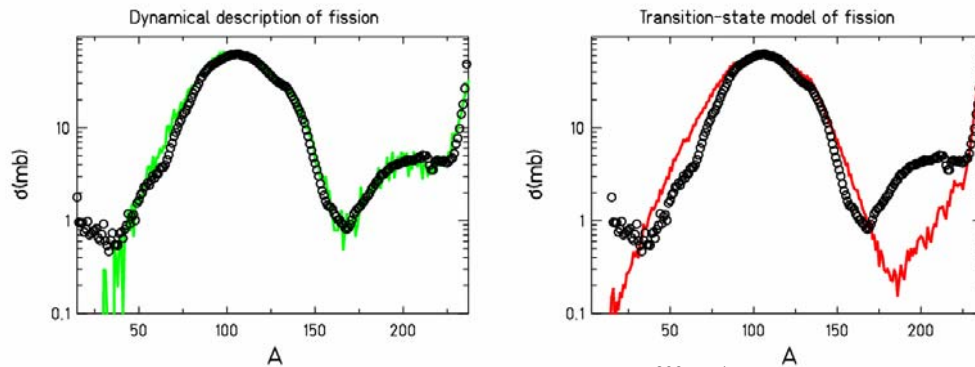


Figure 5: Mass distribution measured in the reaction of $^{238}\text{U}+^1\text{H}$ at 1 A GeV [14,15,20] (open symbols) and compared with two sets of the ABRABLA calculations: left – the proper treatment of the fission process based on the new analytical approximation [37] to the solution of the Fokker-Planck equation, and right – fission width calculated according to the transition-state model [38].

Another point that should be considered in order to have a proper description of the spallation reaction is the energy deposited in the first stage of the reaction. As presented in Ref. [39], the analysis of the isotopic distributions of heavy projectile fragments from the reactions of a ^{238}U beam in a lead target and a titanium target gave evidence that the initial temperature of the last stage of the reaction, the evaporation cascade, is limited to a universal upper value of approximately 5 MeV. The interpretation of this effect relies on the onset of the simultaneous break-up process for systems whose temperature after the first stage of the reaction (e.g. the intra-nuclear cascade) is larger than 5 MeV. In the case of spallation reactions induced by 1 GeV protons, the break-up stage plays an important role for light targets, while for heavy targets only a small fraction of the prefragments in the upper tail of the excitation-energy distribution is formed with temperatures exceeding 5 MeV [40]. As the consequence, the production of intermediate-mass fragments through the simultaneous break-up is more enhanced for light targets (e.g. iron). This could explain the failure of a standard evaporation model to describe the cross section for the production of intermediate-mass fragments (e.g. ^7Be , ^{14}C ...).

Conclusion

In the frame of the HINDAS project, an experimental and theoretical campaign dedicated to the study of the spallation reaction was undertaken at GSI.

The measured data, production cross sections and energies, are of highest interest for the design of accelerator-driven systems. Using the measured production cross sections, combined with the known decay properties, the short- and long-term radioactivities in the target material can be calculated. The number of atomic displacements, being the reason for radiation damages in the structural materials, can now be estimated from the measured kinetic-energy distributions. The data also allow estimating the admixtures of specific chemical elements in the liquid target, accumulated in a long-term operation of the reactor, which enhance the corrosion of the walls or any material in the container.

The systems investigated provide stringent constraints to nuclear-reaction codes, in particular to the modelling of the fission competition and the nuclide production in fission. The new data will help to develop improved models with better predictive power for spallation reactions involving highly fissile nuclei

Acknowledgements

This work was supported by the European commission in the frame of the HINDAS project under the contract number ERBCHBCT940717.

References

-
- [1] <http://www.fynu.ucl.ac.be/collaborations/hindas/>
 - [2] G. Rossi, *Z. Phys.* 82 (1983) 151
 - [3] B.B. Cunningham *et al.*, *Phys. Rev.* 72 (1947) 739
 - [4] R. Wolfgang *et al.*, *Phys. Rev.* 103 (1956) 394
 - [5] E.M. Friedlander *et al.*, *Phys. Rev.* 129 (1963) 1809
 - [6] R. Klapisch, *Ann. Rev. Nucl. Science* 19 (1969) 33
 - [7] H. Sauvageon *et al.*, *Z. Phys. A* 314 (1983) 181
 - [8] M. Gloris *et al.*, *Nucl. Instr. Meth. Phys. Res. A* 463 (2001) 593
 - [9] Yu.E. Titarenko *et al.*, *Phys. Rev. C* 65 (2002) 064610
 - [10] R. Michel, P. Nagel, 1997, *International Codes and Model Intercomparison for Intermediate Energy Activation Yields*, NSC/DOC(97)-1, NEA/OECD, Paris
 - [11] http://www-w2k.gsi.de/kschmidt/nuclear_data.htm
 - [12] W. Wlazole *et al.*, *Phys. Rev. Lett.* 84 (2000) 5736
 - [13] T. Enqvist *et al.*, *Nucl. Phys. A* 686 (2001) 481
 - [14] J. Taieb *et al.*, *Nucl. Phys. A* 724 (2003) 413
 - [15] M. Bernas *et al.*, *Nucl. Phys. A* 725 (2003) 213
 - [16] C. Villagrasa-Canton, PhD thesis, 2003, *Universite de Paris 6, France*
 - [17] L. Audouin, PhD Thesis, 2003, *Universite de Paris 6, France*
 - [18] B. Fernandez-Dominguez, PhD thesis, 2003, *Universite de Caen, France*
 - [19] P. Napolitani, PhD thesis, 2004, *Universite de Paris 6, France*
 - [20] M. V. Ricciardi, PhD thesis, 2005, *University of Santiago de Compostela, Spain*
 - [21] <http://www-w2k.gsi.de/kschmidt/results.htm>
 - [22] M. de Jong *et al.*, *Nucl. Phys. A* 628 (1998) 479
 - [23] T. Enqvist *et al.*, *Nucl. Phys. A* 658 (1999) 47
 - [24] J. Benlliure *et al.*, *Nucl. Phys. A* 638 (2001) 513
 - [25] F. Rejmund *et al.*, *Nucl. Phys. A* 638 (2001) 540
 - [26] P. Chesny *et al.*, *GSI Scientific Rep. 1996, GSI 97-1*, 190
 - [27] A.R. Junghans *et al.*, *Nucl. Instrum. Methods A* 370 (1996) 312
 - [28] B. Jurado *et al.*, *Nucl. Instrum. Methods A* 483 (2002) 630
 - [29] H. Geissel *et al.*, *Nucl. Instrum. Methods B* 70 (1992) 286
 - [30] K.-H. Schmidt *et al.*, *Nucl. Instrum. Methods A* 260 (1987) 287
 - [31] J. Benlliure *et al.*, *Nucl. Instrum. Methods A* 478 (2002) 493
 - [32] A. Kelić *et al.*, *Phys. Rev. C* accepted.
 - [33] D. Morrissey, *Phys. Rev. C* 39 (1989) 460
 - [34] J.-J. Gaimard, K.-H. Schmidt, *Nucl. Phys. A* 531 (1991) 709
 - [35] A. R. Junghans *et al.*, *Nucl. Phys. A* 629 (1998) 635
 - [36] J. Benlliure *et al.*, *Nucl. Phys. A* 628 (1998) 458
 - [37] B. Jurado *et al.*, *Phys. Lett. B* 533 (2003) 186
 - [38] N. Bohr, J. A. Wheeler, *Phys. Rev.* 56 (1939) 426
 - [39] K.-H. Schmidt *et al.*, *Nucl. Phys. A* 710 (2002) 157
 - [40] P. Napolitani *et al.*, *Phys. Rev. C* accepted.